Modeling of fault impacts for a multi-split ductless heat pump system

Howard Cheung, Graduate Research Assistant, Purdue University, West Lafayette, Indiana, US;
James E. Braun, Professor, Purdue University, West Lafayette, Indiana, US

Abstract: In recent years, there is an increasing interest to develop fault detection and diagnostics (FDD) tools for vapor compression systems to avoid degradation of system performance in the field. The effects of multiple types of faults, such as liquid line restriction and condenser fouling, on single-speed systems have been previously studied through both experimental and simulation means. However, little research has been conducted on the fault impacts for multi-split ductless heat pump systems. These systems differ from conventional ducted systems because of the multiple indoor units and complicated control logic associated with compressor speed and electronic expansion valve openings that are used to meet indoor unit loads. In this study, a validated model of a dual-unit multi-split ductless heat pump was used to simulate system performance with one indoor unit subjected to liquid line restriction and electronic expansion valve faults. The simulation results are compared to non-faulted scenarios to examine how the control of the system affects the fault impacts. To assist the development of FDD tools in the future, significant changes of system states with fault levels, such as the superheat and subcooling, are also identified.

Key Words: multi-split heat pump, liquid line restriction, electronic expansion valve fault, simulation

1 INTRODUCTION

Faults for vapor compression systems have been identified as having a major impact on system operation efficiency in recent years, and automated fault detection and diagnostics (FDD) tools are being developed to help technicians to identify these faults and maintain system operation at their designed efficiency. Multiple studies were conducted with various types of vapor compression systems to examine how faults affect their performance and how these effects should be identified using FDD tools. For example, Breuker (1997) tested and simulated a single-speed packaged system with fixed orifice (FXO) under various types of faults: refrigerant leakage, heat exchanger fouling, liquid line restriction and compressor valve leakage. Kim and Kim (2005) tested the effect of compressor faults, heat exchanger fouling and refrigerant leakage on a variable-speed system. Kim *et al.* (2008) did experiments on a single-speed split system controlled by a thermostatic-expansion valve (TXV) with different levels of refrigerant charge, heat exchanger fouling, liquid line restriction, compressor valve leakage and the presence of a non-condensable. Southern California Edison (2009) tested the effect of heat exchanger fouling and charge leakage on a packaged unit and examined the effect of multiple faults on its system performance. Palmiter *et al.* (2011) tested the effect of condenser fouling and charge leakage on the seasonal performance of a heat pump. All these studies showed that faults lead to extra energy usage and change the operating refrigerant temperatures and pressures of the systems. While there have been multiple studies on the effects of faults on systems having a single indoor unit, none of them addressed systems with multiple indoor units. In this paper, a dual-unit ductless heat pump (DHP) system model (Cheung and Braun 2014) was selected as the

baseline model to simulate the impact of liquid line restriction and electronic expansion valve (EEV) faults on system performance when only one of the indoor units is faulted.

2 SYSTEM AND FAULT MODELING

2.1 System model modification

The baseline model (Cheung and Braun 2014) consists of two indoor unit heat exchanger models, an outdoor heat exchanger model, a variable-speed compressor model, an accumulator model, two electronic expansion valve models and five pipeline models to simulate the system performance of an 8000W dual-unit multi-split heat pump with 2.2kg of R410A. The refrigerant-side schematic of the system is shown in Figure 1.

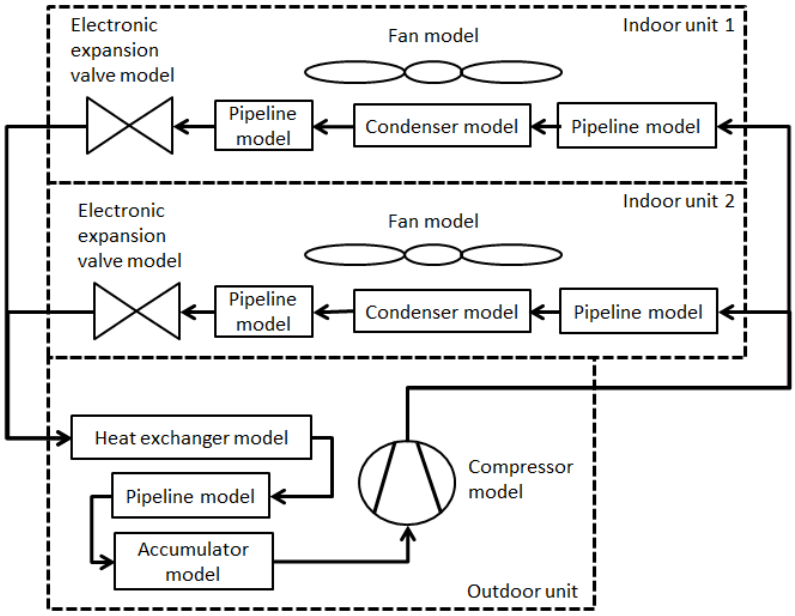


Figure 1: Refrigerant-side schematic of the system model

The baseline model has three control inputs: two valve openings and a compressor speed. The compressor speed ranges from 20Hz to 110Hz and the valve openings of the EEVs span from 27% to 100%. The input-output diagram of the system model is shown in Figure 2.

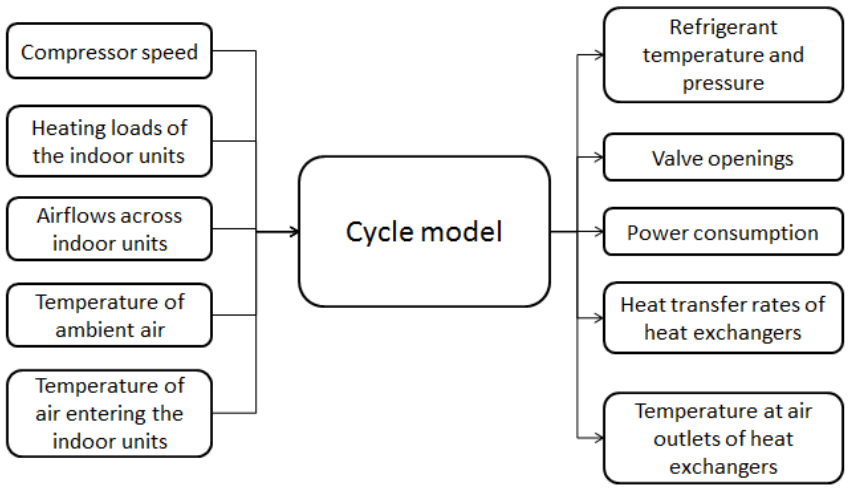


Figure 2: Input-output diagram of the cycle model

The compressor speed in the original model was estimated using an empirical control law derived from experimental results while the valve openings were adjusted to meet required loads for the indoor units. However, in order to simulate the impacts of faults on the system, the control law for compressor speed was changed so that the system operated at the maximum possible coefficient of performance (COP) under non-faulted conditions.

2.1.1 Determination of the compressor speed for optimal COP control

The calculation of compressor speed for a maximum COP was conducted by replacing the empirical control rule for compressor speed in the baseline model with an algorithm that iteratively finds the speed to minimize the power consumption. Since the heating loads of the indoor units are inputs to the cycle model and remain unchanged during the iteration, the minimization is equivalent to the maximization of COP.

2.1.2 Determination of the status of the accumulator

To determine if liquid refrigerant exists in an accumulator, the cycle model in Figure 2 is solved for three different cases as tabulated in Table 1.

Table 1: Different simulation scenarios to determine the status of the accumulator

Case	Fixed variables
A	The charge level inside all components in the system, except the accumulator, is fixed at 2.2kg.
B	The accumulator outlet superheat is fixed at zero.
C	The charge level inside the all components, except the accumulator, is fixed at 2.2kg. The valve openings are fixed as the ones in case B, and the valve openings replace the indoor unit loads in the cycle model in Figure 2 as inputs to the model.

After simulating the cases in Table 1, the validities of cases A and B are checked by examining the state of refrigerant at the accumulator outlet for cases A and C. Case A is valid if the refrigerant at the accumulator outlet is superheated because it is impossible to have two-phase refrigerant at an accumulator outlet in steady state operation for the normal refrigerant charge level of 2.2kg. Case B is only valid if the refrigerant at the accumulator outlet for case C is not superheated. If both cases A and B are invalid, the cycle model in Figure 2 has no solution with the given inputs, and the given compressor speed cannot achieve the required heating loads for the indoor units under the given airflows and environmental conditions. If only one case is valid, the valid case will be accepted as the solution of the cycle model. If both cases are valid, the case that gives the higher COP is accepted as the solution. If case A is accepted, the accumulator does not contain liquid refrigerant. If case B is accepted, the accumulator holds liquid refrigerant and the total mass of refrigerant in the other components is less than 2.2kg.

2.1.3 Final system model

The flowchart of the system model after modification is shown in Figure 3.

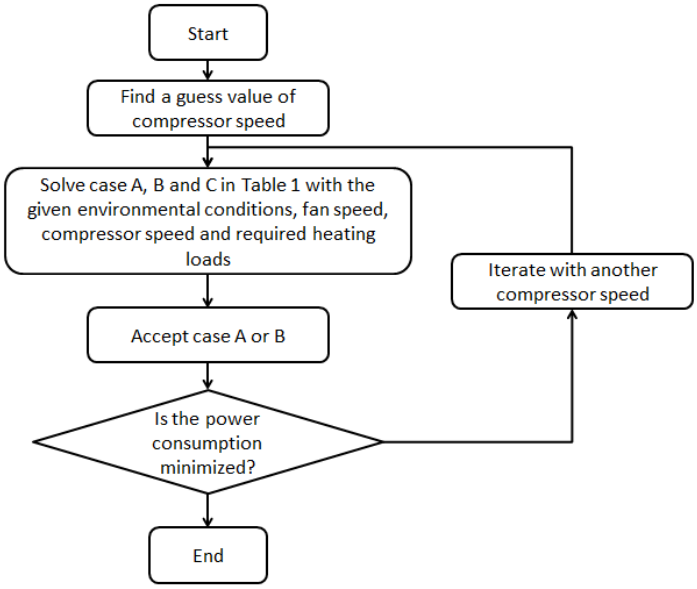


Figure 3: Flowchart to simulate the system performance at maximum COP

Figure 3 shows how the algorithm iterates with different compressor speed to minimize the power consumption. At each iteration, the cases A, B and C listed in Table 1 are solved at the given compressor speed to determine the status of the accumulator. After accepting either case A or B, the COP of the accepted case is examined to see if the given compressor speed maximizes the COP, and the iteration continues until the COP is maximized.

2.2 Fault models

Two fault models are introduced in this paper: liquid line restriction and EEV fault.

2.2.1 Liquid line restriction model

A liquid line restriction is caused by an obstruction in the refrigerant line between the condenser and the expansion valve. It is typically the result of an accumulation of debris within a liquid line filter. The fault causes additional refrigerant pressure drop for the compressor to overcome, and it is simulated by adding a restriction pressure drop to the pressure drop from the component model as shown in Eqn. (1)

$$\Delta P = \Delta P_{model} + \Delta P_{res} \quad (1)$$

where ΔP is the final pressure drop across the liquid line in the faulted case, ΔP_{model} is the pressure drop from the pipeline model and ΔP_{res} is the restriction pressure drop

2.2.2 EEV fault

In this study, a stuck EEV was considered as a fault where the valve opening is fixed at a certain position. The simulation procedure used to consider a fixed valve opening was documented in Cheung and Braun 2014. With one less degree of freedom, there is no opportunity to maximize COP and the compressor speed and opening of the non-faulted EEV are adjusted to achieve the required heating loads of the two indoor units.

3 RESULTS AND DISCUSSION

3.1 Non-faulted conditions

To examine the effects of liquid line restriction and stuck EEV, a range of indoor loads for the non-faulted scenarios described in Table 2 were simulated for comparison.

Table 2: Inputs for the non-faulted condition

Indoor room temperature [°C]	21.1
Outdoor room temperature [°C]	8.67
Airflow across indoor units [m^3/s]	0.1764
Heating load of indoor unit 1 [W]	1700 to 4000
Heating load of indoor unit 2 [W]	3500

The compressor speed and valve openings for the indoor load scenarios in Table 2 are plotted in Figure 4, and the associated changes of subcooling, superheat and COP are shown in Figure 5.

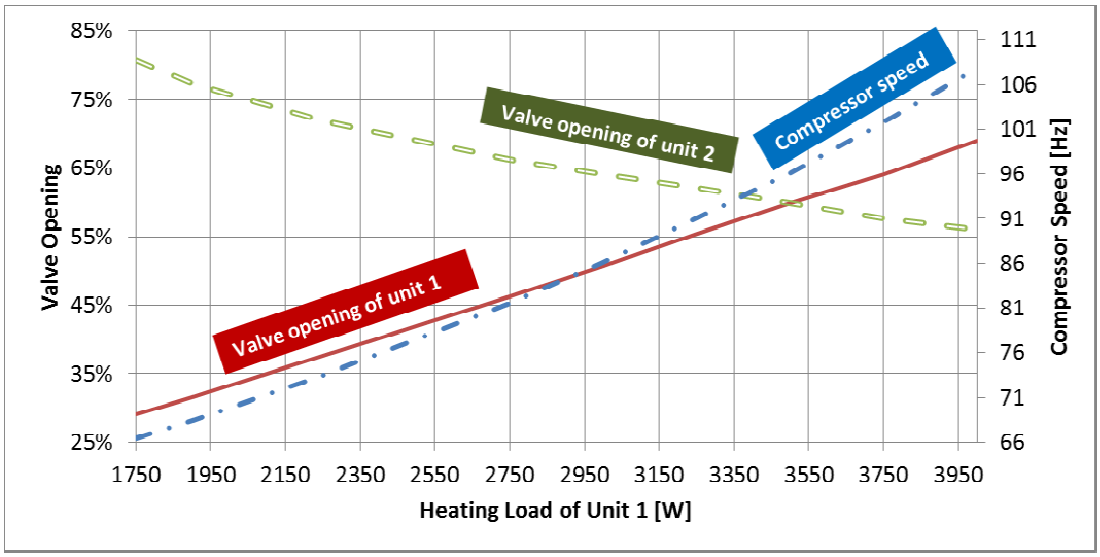


Figure 4: Changes of valve openings and compressor speed with increasing heating load of unit 1

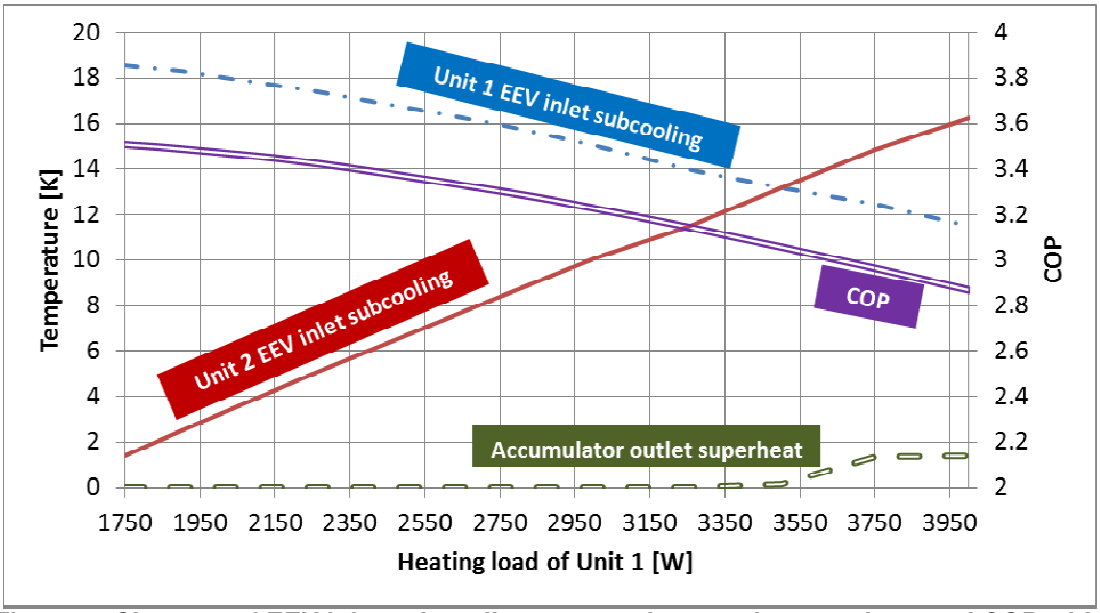


Figure 5: Changes of EEV inlet subcooling, accumulator outlet superheat and COP with increasing heating load of unit 1

Figure 4 shows that when the heating load of unit 1 increases from 1750W, the valve opening of unit 1 increases. The compressor speed also rises to meet the higher total heating load. With a constant heating load of unit 2, the load ratio of unit 2 (the ratio of indoor unit load to the total heating load) decreases and the valve opening of unit 2 decreases because of the greater compressor speed. The change of control inputs, as shown in Figure 5, results in decreases of COP and subcooling at the inlet of EEV of unit 1 and an increase of subcooling at the inlet of EEV of unit 2. When the heating load of unit 1 reaches 3500W, liquid refrigerant in the accumulator has vaporized completely, and the accumulator outlet superheat increases with the increasing load. Beyond the range of heating loads of unit 1 in Table 2, either the compressor speed saturates at its maximum or the valve opening of unit 1 saturates at its minimum, and the system varies the remaining unsaturated compressor speed or valve openings to reach the required heating load.

3.2 Liquid line restriction

The effect of liquid line restriction on system performance is studied by imposing different levels of liquid line restriction on indoor unit 1 only to the non-faulted scenario with a heating load of indoor unit 1 of 3500W. The change of valve openings and compressor speed with increasing liquid line restriction level is shown in Figure 6, and the changes of subcooling, superheat and COP are shown in Figure 7.

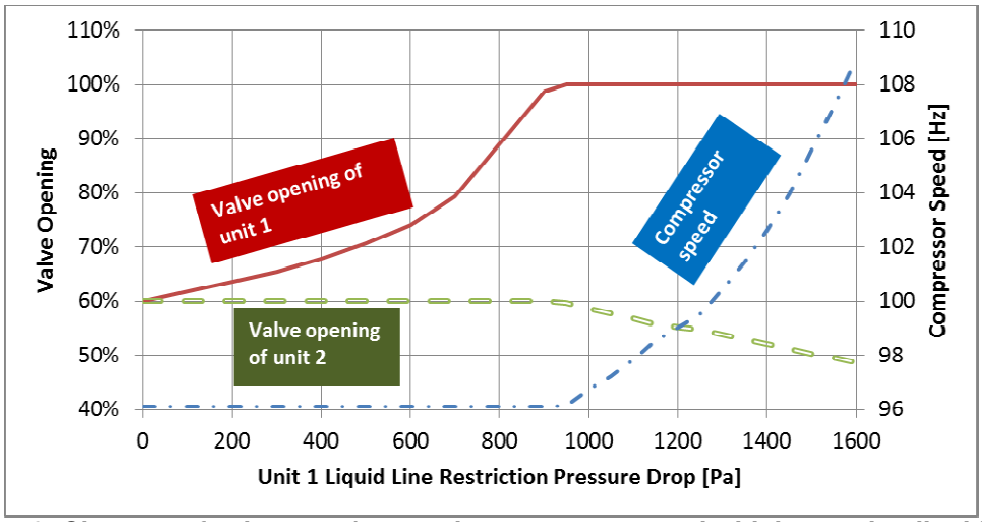


Figure 6: Changes of valve openings and compressor speed with increasing liquid line restriction on unit 1

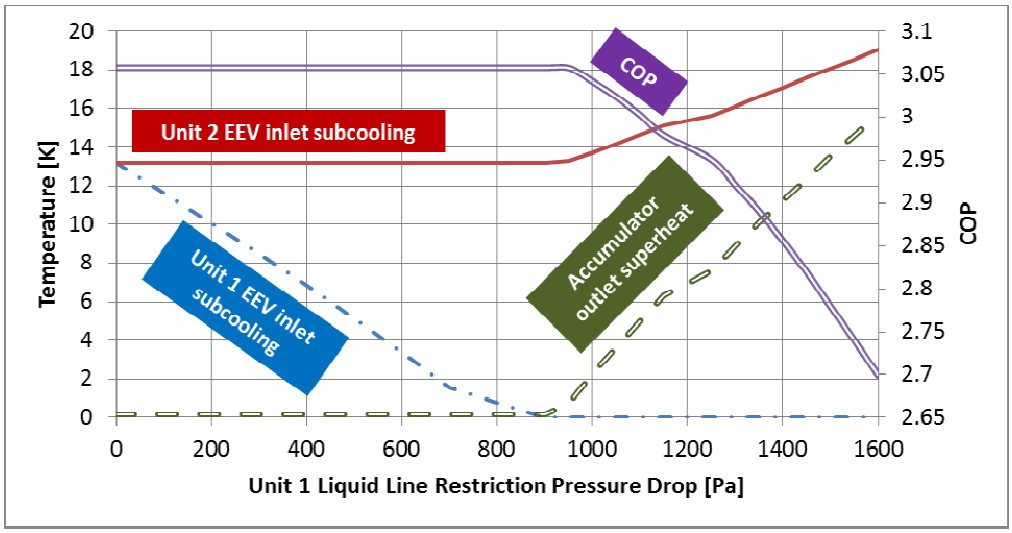


Figure 7: Changes of EEV inlet subcooling, accumulator outlet superheat and COP with increasing liquid line restriction on unit 1

Figure 6 shows that when a relatively small liquid line restriction is considered in unit 1, the valve opening of the faulted indoor unit increases to compensate for the fault and the fault has no effect on COP as shown in Figure 7. However, when the restriction pressure drop reaches 950Pa, the valve opening of unit 1 has reached maximum and the valve cannot be used to control the heating load of unit 1. With a saturated valve opening of unit 1, optimal control for COP cannot be achieved and the compressor speed and the valve opening of unit 2 are controlled to satisfy the heating load requirement of both units with increasing liquid line restriction. The increase of speed and decrease of the valve opening cause a drop of COP, an increase in accumulator outlet superheat and an increase of valve inlet subcooling of unit 2. At a liquid line restriction of 1600Pa, the compressor speed approaches the maximum compressor speed of 110Hz. When the maximum compressor speed is reached with a higher liquid line restriction, the system cannot maintain the heating load requirement of both indoor units because both the compressor speed and the valve opening of unit 1 are saturated.

3.3 EEV fault on the unit with changing heating load

To examine how a stuck EEV fault for one indoor unit affects the system performance over a range of loads, a constant valve opening for unit 1 of 60% was assumed with the scenario in Table 2. This valve position corresponds to the non-faulted position for an indoor unit 1 heating load of 3500W. The change of compressor speed and valve openings of the faulted system at different heating loads for unit 1 is plotted in Figure 6.

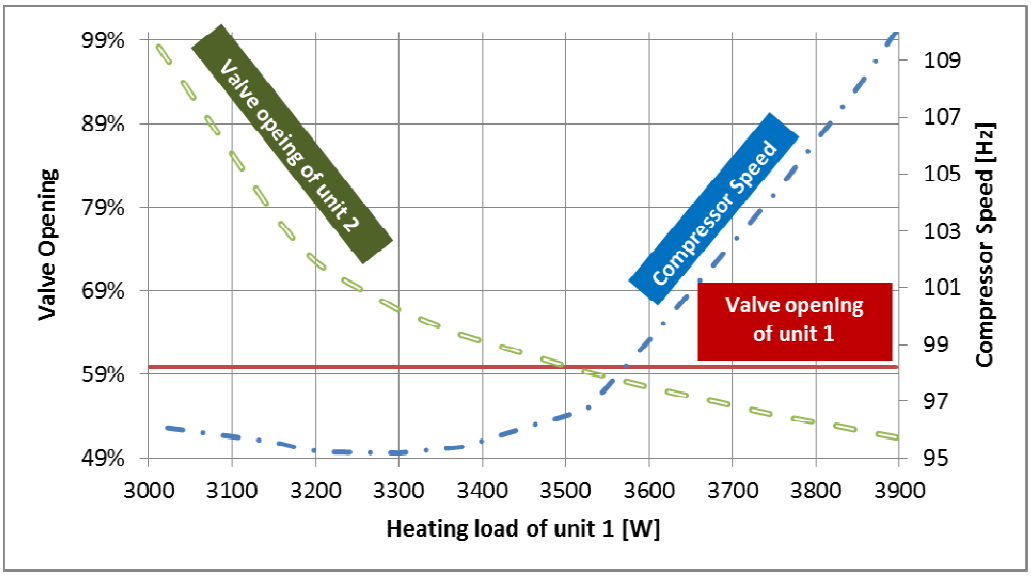


Figure 8: Change of valve openings and compressor speed with increasing heating load of unit 1 when valve of unit 1 is faulted

Figure 8 shows an increase of compressor speed and decrease of valve opening of unit 2 similar to the non-faulted case in Figure 4 when the heating load of unit 1 is higher than 3300W. However, the changes in Figure 8 are more significant than Figure 4 in that the valve opening of unit 2 saturates at its maximum when the load is 3000W and the compressor speed saturates at its maximum when the load is 3900W. With a faulted EEV in unit 1, the system cannot achieve the required heating loads when the heating load of unit 1 lies outside the range between 3000W and 3900W. Compared to the non-faulted scenario in Figure 4, the range of achievable heating loads of the system becomes smaller when the valve is faulted.

One major difference between Figure 8 and Figure 4 is that the compressor speed increases with decreasing heating load when the heating load is lower than 3300W in Figure 8. This can be explained by the change of compressor suction superheat in Figure 9.

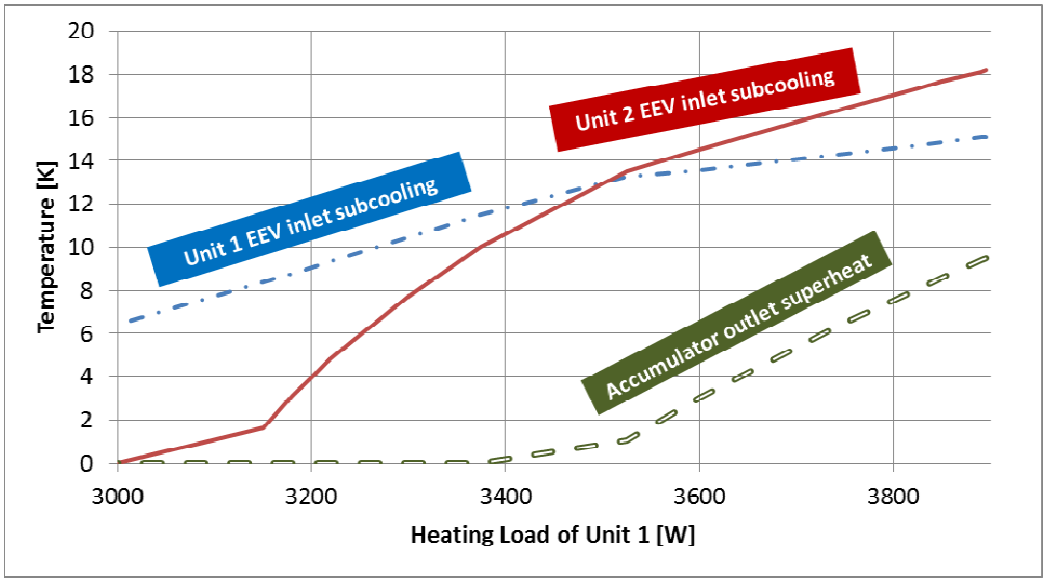


Figure 9: Change of EEV subcooling and accumulator outlet superheat with increasing heating load of unit 1 when valve of unit 1 is faulted

Figure 9 shows that the accumulator outlet superheat is zero and the accumulator holds liquid refrigerant when the heating load of unit 1 is lower than 3300W. With a decreasing heating load of unit 1, the valve opening of unit 2 increases to satisfy the increasing load ratio of unit 2. The increase in valve opening leads to liquid refrigerant entering the accumulator and reduces the effective charge level in the system. This reduces the subcooling and hence the refrigerant flow across unit 2 significantly. In order to maintain a refrigerant flow in unit 2 to support its heating load, the compressor speed increases in response to the decreasing heating load of indoor unit 1 with liquid refrigerant in the accumulator.

The COP in the faulted scenario is compared to the non-faulted case in Figure 10.

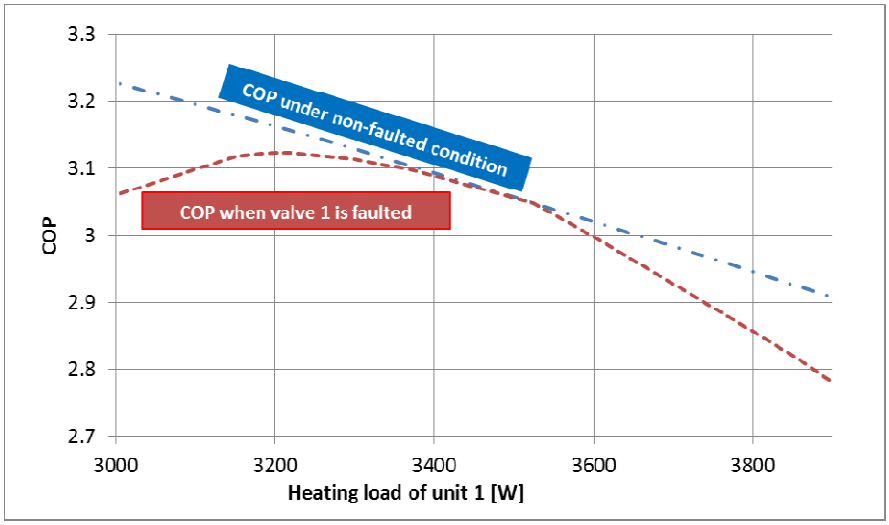


Figure 10: Change of COP with increasing heating load of unit 1 under non-faulted condition and the case with a faulted EEV in unit 1

Figure 10 shows that the COP for non-faulted condition is higher than or equal to the ones in the faulted scenario. At the heating load of unit 1 of 3500W, the performance of the faulted

and non-faulted scenarios is the same because they have the same valve openings. However, while the non-faulted system can implement optimal COP control in the range of heating loads in Figure 10, the faulted system cannot vary the valve opening of unit 1 to maximize its COP and operates with a lower COP. As the heating load of unit 1 shifts from 3500W, the difference between their control inputs grows, and the difference between their COPs increases as shown in Figure 10.

3.4 EEV fault on the unit with constant heating load

The EEV of unit 2 was fixed at 60% and performance was simulated for the scenarios in Table 2 with increasing load for unit 1 and constant load for unit 2. The compressor speed and valve openings in this faulted scenario are shown in Figure 11.

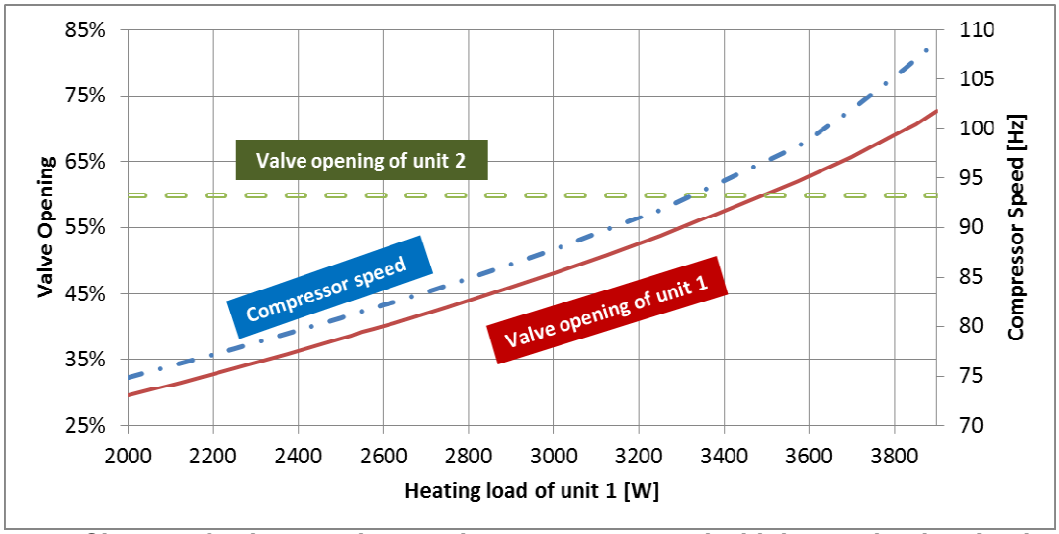


Figure 11: Change of valve openings and compressor speed with increasing heating load of unit 1 when the EEV of unit 2 is faulted

Figure 11 shows that when the EEV of unit 2 is faulted and the heating load of unit 1 increases, both the valve opening of unit 1 and compressor speed increase to achieve the increasing total heating load. The valve opening of unit 1 reaches its minimum when the load drops to 2000W and the compressor speed is saturated at its maximum when the load reaches 3900W. The faulted system does not have enough degrees of freedom to fulfill the heating loads of the units when the heating load of unit 1 lies outside the range between 2000W and 3900W. Similar to the case in section 3.3, the EEV fault limits the range of heating loads that the system can achieve.

The impact of the EEV fault on the EEV inlet subcooling and accumulator outlet superheat are plotted in Figure 12.

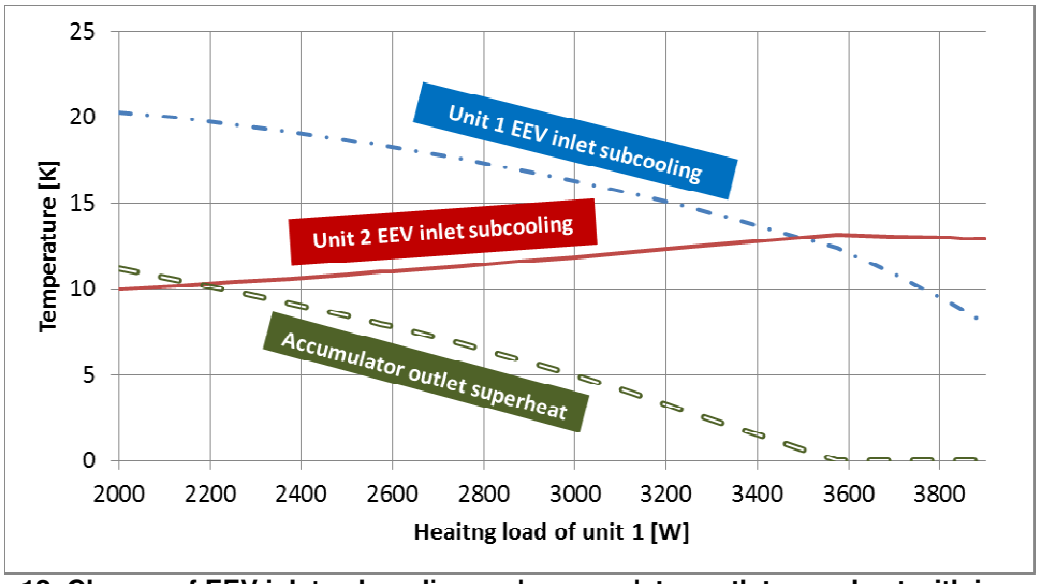


Figure 12: Change of EEV inlet subcooling and accumulator outlet superheat with increasing heating load of unit 1 when the EEV of unit 2 is faulted

As the heating load of unit 1 increases from 200W in Figure 12, the accumulator outlet superheat and the inlet subcooling of the EEV of unit 1 decrease, and the inlet subcooling of the EEV of unit 2 increases. When the superheat falls to zero at the heating load of unit 1 of 3600W, liquid refrigerant accumulates in the accumulator and the effective charge level of the system drops. This causes a decrease of subcooling of the EEV of unit 2 when the heating load of unit 1 increases from 3600W.

The COPs between the faulted and the non-faulted scenarios are compared in Figure 13.

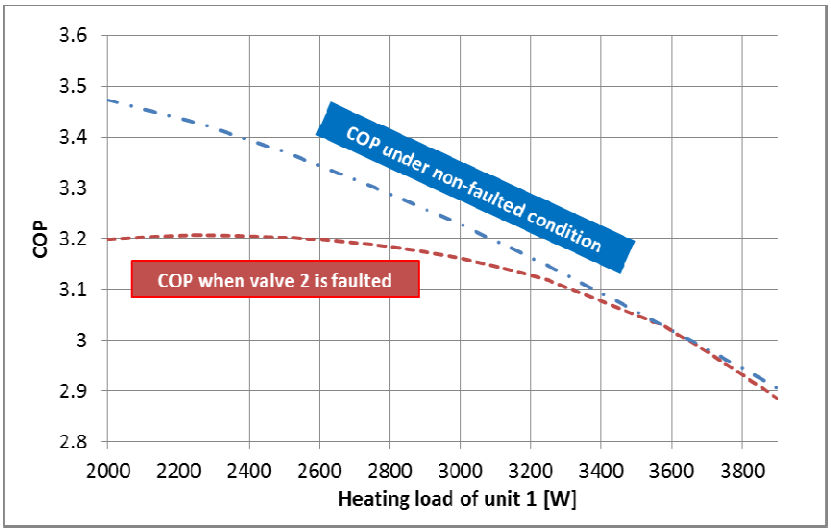


Figure 13: Change of COP with increasing heating load of unit 1 under non-faulted condition and the case with a faulted EEV in unit 2

Figure 13 shows that the COP of the non-faulted system is higher than or equal to the COP of the system with a faulted EEV in unit 2. At a heating load of unit 1 of 3500W, the valve openings of unit 2 in both scenarios are the same and they have the same COP. However, as the load shifts from 3500W, the difference of the control inputs between the two cases grows. While the non-faulted system has enough degrees of freedom to maximize its COP and reach the heating loads simultaneously, the valve opening of unit 2 in the faulted system

is locked and the faulted system cannot achieve maximum COP. This creates a growing difference between the two COPs as the heating load of unit 1 deviates from 3500W.

4 CONCLUSIONS

This paper demonstrated how to create a dual-unit DHP system model with optimal COP control from an existing dual-unit DHP system model by changing the algorithm to determine its compressor speed and the status of the refrigerant in the accumulator.

The paper also showed how a liquid line restrictions and stuck EEV for an indoor unit in a dual-unit DHP system affect system performance. A small liquid line restriction can be compensated for by the EEV control in the faulted unit. However, a significant liquid line restriction that leads to saturation of the valve opening can result in an increase of compressor speed, accumulator outlet superheat and subcooling of the non-faulted units and a decrease of COP. When a serious liquid line restriction causes saturation of compressor speed and valve opening of the faulted unit, the system will lose its ability to meet all the heating loads of its indoor units.

A stuck EEV deteriorates system COP and shrinks the range of achievable heating loads of a dual-unit DHP system. When an EEV opening is fixed, the system does not have enough degrees of freedom to achieve maximum COP. The faulted system operates with a different compressor speed and valve openings than the optimal scenario in order to meet the heating loads, and the COP becomes lower than that of the non-faulted system. This also speeds up the saturation of other control inputs (i.e. compressor speed and valve opening of non-faulted valves) and reduces the range of achievable heating loads of the system.

5 REFERENCES

Breuker M. S. 1997. Evaluation of a statistical, rule-based detection and diagnostics method for vapor compression air conditioners, Master's thesis, Purdue University, West Lafayette

Cheung H. and Braun J. E. 2014. "Component-based, gray-box modeling of ductless multi-split heat pump systems," *International Journal of Refrigeration*, Vol 38, pp 30 - 45

Kim M. and Kim M. S. 2005 "Performance investigation of a variable speed vapor compression system for faulted detection and diagnosis," *International Journal of Refrigeration*, Vol 28, pp 481 - 488

Kim M., Yoon S. H., Domanski P. A. and Payne W. V. 2008 "Design of a steady-state detector for fault detection and diagnosis of a residential air conditioner," *International Journal of Refrigeration*, Vol 31, pp 790 - 799

Palmiter L., Kim J., Larson B., Francisco P. W., Groll E. A. and Braun J. E. 2011 "Measured effect of airflow and refrigerant charge on the seasonal performance of an air-source heat pump using R410A," *Energy and Buildings*, Vol 43, pp 1802 - 1810

Southern California Edison. 2009. Report ETO 08.02 - 08.09